

# Formation of conversion Zn-Ni-Mn phosphate coatings on steel and corrosion behaviour of phosphated specimens in a chloride-contaminated alkaline solution

O. Girčienė\*,

R. Ramanauskas,

L. Gudavičiūtė,

A. Martušienė

*Department of Electrochemical  
Materials Science, Institute  
of Chemistry, Centre for Physical  
Sciences and Technology,  
A. Goštauto 9, LT-01108 Vilnius,  
Lithuania*

The formation of the crystalline Zn-Ni-Mn phosphate coating on carbon steel as well as the protective abilities of this coating in a chloride contaminated alkaline solution have been studied. The chemical composition and the morphology of the phosphate coating were evaluated by the X-ray diffraction and scanning electron microscopy techniques. The gravimetric study has shown that the formed phosphate coating (0.4 at.% of Ni and 1.1 at.% of Mn) was medium weight ( $1.9\text{--}3.4\text{ g m}^{-2}$ ) with the thickness of  $\sim 2\text{ }\mu\text{m}$ . According to XRD analysis data the coating was composed of three phases: hopeite  $\text{Zn}_3(\text{PO}_4)_2 \cdot 4\text{H}_2\text{O}$ , phosphophyllite  $\text{Zn}_2\text{Fe}(\text{PO}_4)_2 \cdot 4\text{H}_2\text{O}$  and Fe. The results of electrochemical measurements revealed that after immersion into a saturated  $\text{Ca}(\text{OH})_2 + 1\text{ M NaCl}$  solution for 1 h the corrosion current  $i_{\text{corr}}$  of phosphated samples decreased about twenty-fold and the polarization resistance  $R_p$  increased seventeen-fold as compared to those of the substrate. The prolongation of exposure time of phosphated samples to the solution up to 15 days leads to an approximately thirty-fold increase in  $R_p$  values as compared to those obtained for bare steel. Therefore, the low porosity ( $\sim 1\%$ ) medium weight crystalline Zn-Ni-Mn phosphate coating on carbon steel demonstrated effective protective properties in a chloride-contaminated alkaline solution.

**Key words:** carbon steel, phosphate coating, corrosion, resistance

## INTRODUCTION

In concrete systems the corrosion of reinforcing steel rebars has gained considerable attention [1–3]. The corrosion resistance of rebars can be increased either by modifying the chemical composition of steel rebars or by applying metallic (galvanized steel) or organic (epoxy-coated rebar, oil) coatings on the surface of such rebars. Among the possible anti-corrosion methods, phosphated reinforcing bars could be employed to extend the lifetime of the rebars in concrete structures [2, 4]. As an important surface treatment method, phosphating has become so popular that it has been used on Fe and steel, Al and Zn alloys, Cd, as well as other metal ma-

terials [5]. The protective film formed on the metal surface consists mainly of metal oxides and phosphate. The process of its formation occurs through a dissolution-precipitation mechanism and its growth rate is controlled by the solution resistance in pores [3, 5].

In order to obtain high quality phosphate coatings, many researchers have focused on the improvement of the quality of these phosphate coatings through the use of ions, such as  $\text{Ni}^{2+}$  and  $\text{Mn}^{2+}$  [6–10]. The presence of  $\text{Ni}^{2+}$  ions in the phosphating bath improves the corrosion resistance at the base of pores [11, 12] and accelerates the surface reactions during phosphating [13]. Addition of  $\text{Mn}^{2+}$  ions to the bath improves the corrosion resistance and decreases the porosity by formation of a dense and fine microstructure [14, 15]. Furthermore, the literature data show that the elements such as Ni and Mn

\* Corresponding author. E-mail: olgag@chi.lt

increase the alkaline stability of phosphate coatings [2, 10, 16, 17]. The authors [16, 17] have measured the rate of Zn, Mn and Ni phosphates leaching during exposure to an alkaline electrolyte. The results obtained demonstrate the importance of Mn in increasing the alkaline resistance of the phosphate layer. By contrast, the effect of Ni on the alkaline resistance is significantly less, reflecting its lower incorporation into the phosphate crystal lattice. It has been proposed that the presence of  $\text{Ni}^{2+}$  in the phosphate bath increases the alkaline resistance of the top layer [16].

One problem in use of the phosphate coatings in aggressive media is the existence of open pores and pinholes [18–21]. The pores provide a path for corrosion attack, leading to localised corrosion in an aggressive environment. The corrosion resistance of the phosphate coating is related to the size and population density of pores in the film. As the corrosion reactions are initiated at the coating-substrate interface, determination of porosity is important to estimate the overall corrosion resistance of the coated materials [20].

The aim of the present work was to study the formation of an environment-friendly, alkaline resistant conversion Zn-Ni-Mn phosphate coating on carbon steel as well as to investigate the protective characteristics of this coating in a chloride contaminated alkaline solution.

## EXPERIMENTAL

### Substrate and coating

Analytical grade chemicals were used to deposit the trication Zn-Ni-Mn phosphate coating and to prepare a testing solution. Carbon steel samples with an area of  $60 \text{ cm}^2$  were used for phosphating (Table 1). Surface pre-treatment included alkaline degreasing and water rinsing prior to phosphating without any special surface activation.

The weight of phosphate coating ( $p_{\text{ph}}$ ) and the mass of dissolved metal ( $p_{\text{Me}}$ ) were calculated from gravimetric measurements. The samples were weighed after surface degreasing, after phosphate coating deposition and after removal of the phosphate coating in a 25% solution of  $\text{CrO}_3$  ( $t^\circ = 70 \text{ }^\circ\text{C}$ ,  $t = 2 \text{ min}$ ). The accuracy of weighing was  $\pm 0.0001 \text{ g}$ . The data on weights of the phosphate coating, the potential values were average from three to five measurements.

The variation in the pH value in a “thin layer” of the solution was studied in a special cuvette with a volume of  $1.8 \text{ cm}^3$  into which a specimen with a surface area of  $60 \text{ cm}^2$  was im-

mersed. The “thin layer” thickness was 0.3 mm. The pH value was measured by using a pH-673 meter with an ESL-41-115-01 standard glass electrode and a gage for micro measurements during no longer than 15 s upon phosphating. Three parallel measurements were performed. The correlation coefficient was 0.95–1.00.

### Surface analysis

The morphology and elemental composition of the phosphate coating were studied by a scanning electron microscope (SEM) EVO 50 EP (Carl Zeiss SMT AG) with an INCA energy disperse X-ray spectrometer (Oxford Instruments).

The phases in the phosphate coating were determined by X-ray diffraction (XRD) measurements, which were performed with a diffractometer D8 Advance (Bruker AXS) equipped with a Göbel mirror (primary beam monochromator) for Cu radiation ( $\lambda = 0.154183 \text{ nm}$ ). The step-scan mode was used in the  $2\Theta$  ranges from  $xx^\circ$  to  $yy^\circ$  with a step-length of  $0.04^\circ$  and a counting time of 5 s per step.

### Electrochemical measurements

The corrosion behaviour of phosphated carbon steel was investigated in an aerated stagnant saturated  $\text{Ca}(\text{OH})_2$  solution containing 1 M NaCl. The electrolyte was prepared from analytical grade chemicals and deionized water. All the experiments were performed at ambient temperature.

The working electrodes were carbon steel samples the composition of which is listed in Table 1, with an area of  $4 \text{ cm}^2$ , covered with the phosphate layer (Table 2). The phosphated samples were kept for 3 days under ambient conditions prior to the measurements.

All electrochemical measurements were performed with an Autolab PGSTAT302 potentiostat using a standard three-electrode system with a Pt counter electrode and a saturated Ag/AgCl reference electrode. All potentials are reported versus a saturated Ag/AgCl reference electrode. Before experiments, the open circuit potential ( $E_{\text{corr}}$ ) of electrodes in the solution was monitored for 0.5 h. The data on  $E_{\text{corr}}$  values were average of five measurements. The corrosion current densities ( $i_{\text{corr}}$ ) were determined by Tafel line extrapolation. One specimen was used for a measurement, with the potential scan of  $0.5 \text{ mV s}^{-1}$ , from cathodic to anodic region. The polarization resistance ( $R_p$ ) values were determined from liner polarization measurements, which were performed between  $\pm 10 \text{ mV}$  around  $E_{\text{corr}}$ , after an immersion for 1 h in the base

Table 1. Chemical composition of steel (wt.%)

| Elements    | C    | Mn  | Si  | Cr         | Ni      | Cu      | P        | S         |
|-------------|------|-----|-----|------------|---------|---------|----------|-----------|
| Composition | 0.21 | 1.2 | 0.6 | $\leq 0.3$ | $< 0.3$ | $< 0.3$ | $< 0.04$ | $< 0.045$ |

Table 2. Coating weight, thickness and elemental composition of the phosphate coating

| Sample   | Coating thickness, $\mu\text{m}$<br>(by XRD) | Coating weight,<br>$\text{g m}^{-2}$ | Elements, at. % (by EDS) |     |     |     |      |      |
|----------|--|--------------------------------------|--------------------------|-----|-----|-----|------|------|
|          |  |                                      | Zn                       | Ni  | Mn  | Fe  | O    | P    |
| Zn-Ni-Mn | 1.7–1.9                                      | 2.9–3.4                              | 9.9                      | 0.4 | 1.1 | 9.8 | 67.5 | 11.3 |

solution, with a scan rate of  $0.1 \text{ mV s}^{-1}$ . The measurements of electrochemical impedance spectra (EIS) were performed at the open circuit potential with the FRA2 module applying a signal of  $10 \text{ mV}$  amplitude, in the frequency range of  $20 \text{ kHz}$  to  $0.001 \text{ Hz}$ .

## RESULTS AND DISCUSSION

### The growth of the phosphate coating

When a metal surface is immersed in the phosphating bath, the etching attack is initiated by free phosphoric acid, and metals ions and hydrogen are generated [2–4].



Near the metal surface, the solution is alkalinized, and an insoluble phosphates deposit is formed at the metal surface. The acidity of the bath is of high importance. It is an equilibrium bath that provides the maximum phosphating rate and minimum weight loss of the phosphated metal. The dependences of the gain in weight of phosphate film ( $p_{\text{Ph}}$ ) and the weight of etched metal ( $p_{\text{Me}}$ ) values on the solution pH

are presented in Fig. 1a. The phosphating regime is optimal when  $p_{\text{Ph}}$  and  $p_{\text{Me}}$  reach their constant values and the ratio  $K_{\text{ef}} = p_{\text{Ph}}/p_{\text{Me}}$  reaches its maximum value. The data in Fig. 1a testify that at  $\text{pH} = 3.4\text{--}3.6$   $K_{\text{ef}}$  acquires its constant maximum value equal to  $\sim 4.8$ . The “thin layer” method makes it possible to follow the variation in solution pH in the near-surface layer during phosphating. The studied dependency of the change of pH ( $\Delta\text{pH}$ ) solution after deposition of insoluble phosphates ( $\text{pH}_{\text{dep}}$ ) on pH prior to phosphating ( $\text{pH}_0$ )  $\Delta\text{pH} = \text{pH}_{\text{dep}} - \text{pH}_0$  is linear (Fig. 1b). Figure 1c shows the influence of the concentration of  $\text{NO}_3^-$  ions on the main characteristics of phosphating, such as  $p_{\text{Ph}}$  and  $p_{\text{Me}}$ . The optimum value of  $\text{pH} = 3.4$  was determined in accordance with the data presented in Fig. 1a. As is evident from Fig. 1c, at  $c_{\text{NO}_3^-} = 0.1$ , M  $p_{\text{Ph}}$  and  $p_{\text{Me}}$  reach their maximum values. Figure 1d illustrates the dependence of  $p_{\text{Ph}}$  and  $p_{\text{Me}}$  on phosphating time in the solution of optimum composition. There is a rapid growth period of phosphate coating weight in the initial period. When the phosphate coating covers the most of steel surface, the growth rate of the coating weight tends to slowdown.

There is a relation between coating density and its weight of about  $1 \mu\text{m}$  corresponding to  $1.5\text{--}2 \text{ g m}^{-2}$  for most phos-

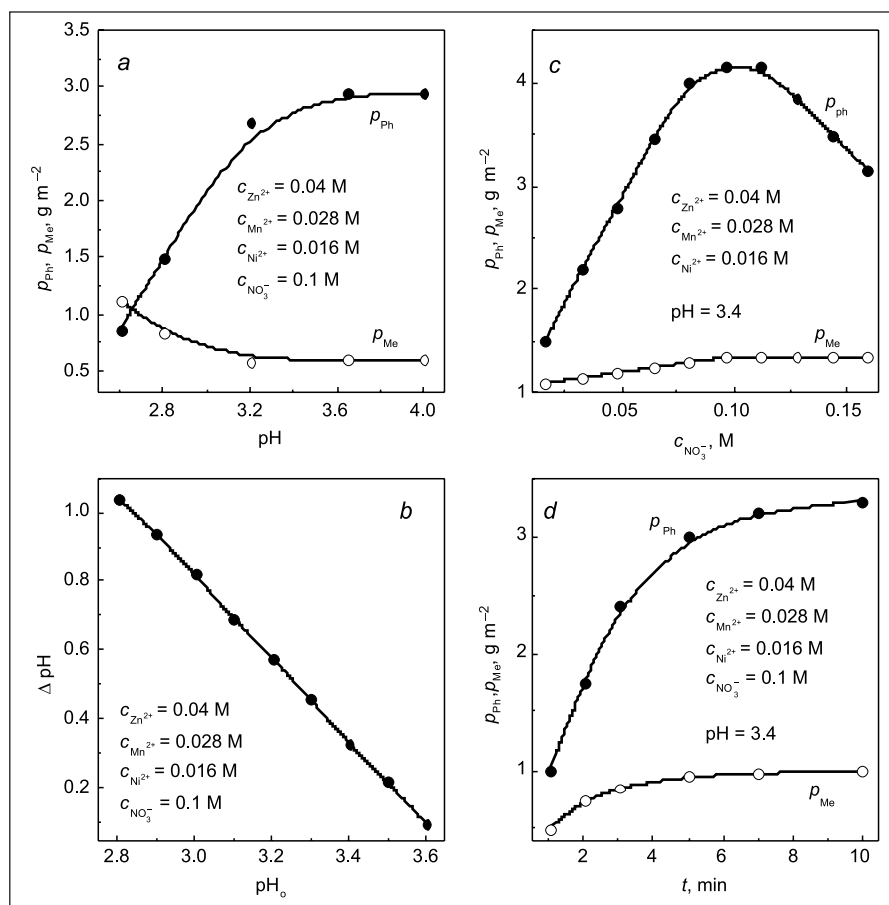


**Fig. 1.** a – Dependence of the Zn-Ni-Mn phosphate coating weight  $p_{\text{Ph}}$  and the mass of dissolved metal  $p_{\text{Me}}$  on pH of the solution, phosphating time  $t = 10 \text{ min}$ . b – Dependence of difference in solution pH ( $\Delta\text{pH}$ ) after deposition of the coating on the initial solution pH ( $\text{pH}_0$ ),  $t = 10 \text{ min}$ . c – Dependence of  $p_{\text{Ph}}$  and  $p_{\text{Me}}$  on the concentration of  $\text{NO}_3^-$  ions in the solution,  $t = 10 \text{ min}$ . d – Dependence of  $p_{\text{Ph}}$  and  $p_{\text{Me}}$  on  $t$

phosphate coatings [10]. The gravimetric measurements showed that the phosphate coating studied can be classified as medium weight ( $1.9\text{--}3.4\text{ g m}^{-2}$ ) ones with the thickness of  $\sim 2\text{ }\mu\text{m}$  (Table 2). Normally, medium weight ( $1.4\text{--}7.5\text{ g m}^{-2}$ ) phosphate coatings demonstrate a crystalline structure [10].

For all subsequent experiments the phosphating solution of the following composition was used:  $\text{Zn}^{2+} - 0.04\text{ M}$ ,  $\text{Mn}^{2+} - 0.028\text{ M}$ ,  $\text{Ni}^{2+} - 0.016\text{ M}$ ,  $\text{PO}_4^{3-} - 0.26\text{ M}$ ,  $\text{NO}_3^- - 0.1\text{ M}$ ,  $\text{pH} = 3.2\text{--}3.6$ ,  $t = 50\text{--}55\text{ }^\circ\text{C}$ ,  $10\text{ min}$ .

### Morphology and composition

The best protection of the substrate is achieved when a uniform fine crystalline layer covers the surface. The SEM observations show that the Zn-Ni-Mn phosphate coating is compact, well crystallized and completely covers the steel surface (Fig. 2). The structure is characterized by right-angled crystallites with a width of about  $0.2\text{ }\mu\text{m}$  and a length of  $2\text{ }\mu\text{m}$ . The XRD analysis performed on the coated steel indicates the presence of three phases: hopeite  $\text{Zn}_3(\text{PO}_4)_2 \cdot 4\text{H}_2\text{O}$ , phosphophyllite  $\text{Zn}_2\text{Fe}(\text{PO}_4)_2 \cdot 4\text{H}_2\text{O}$  and metallic Fe (Fig. 3). The

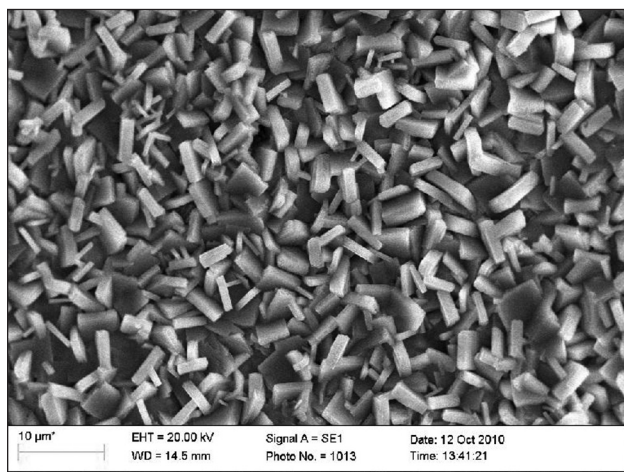


Fig. 2. A SEM micrograph of the Zn-Ni-Mn phosphate coating on carbon steel

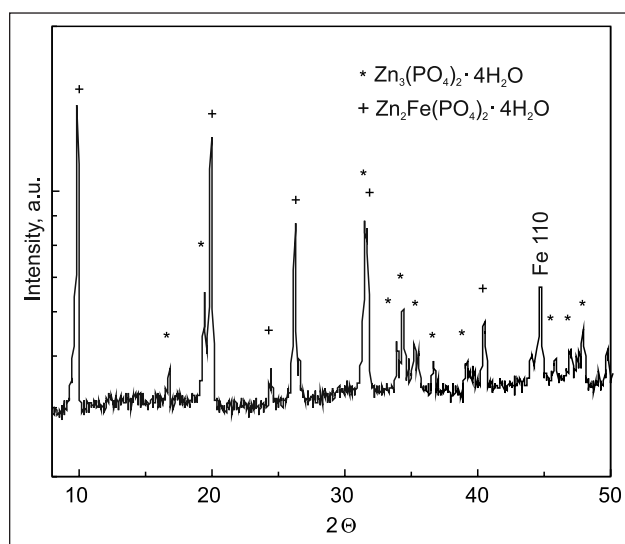
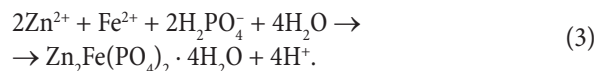
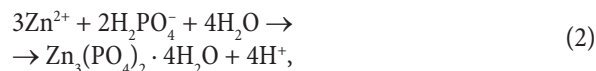


Fig. 3. XRD pattern of the Zn-Ni-Mn phosphate coating on carbon steel

presence of the phosphophyllite phase is related to the carbon steel dissolution in the acid bath ( $\text{pH} = 3.2\text{--}3.6$ ) during the phosphate treatment [5]. According to [13], the possible reactions for the hopeite and phosphophyllite formation are the following:



The intensities of diffraction lines are proportional both to the volume fraction of the phosphate phase and the thickness of the phosphate layer [22]. Therefore, the comparison of the intensities of metallic Fe diffraction lines of samples without / with the phosphate layer suggests that the thickness of the trication phosphate coating formed on the surface of carbon steel is  $\sim 2\text{ }\mu\text{m}$  (Table 2).

The analysis of elemental composition of the phosphate coating was performed by EDS measurements, the results of which are listed in Table 2 and indicate that the Zn-Ni-Mn coating contains  $0.4\text{ at.}\%$  of Ni and  $1.1\text{ at.}\%$  of Mn.

### Corrosion behaviour

#### Corrosion potential evolution

In as much as chloride ions promote steel corrosion, the electrochemical measurements were performed in a saturated  $\text{Ca}(\text{OH})_2 + 1\text{ M NaCl}$  solution (base). The variation in  $E_{\text{corr}}$  values for unphosphated and phosphated carbon steel samples in the base solution is shown in Fig. 4. The most rapid evolution of  $E_{\text{corr}}$  occurred within  $\sim 30\text{ min}$  of the sample immersion, while further potential evolution was slower and did not change significantly. Therefore,  $E_{\text{corr}}$  values were

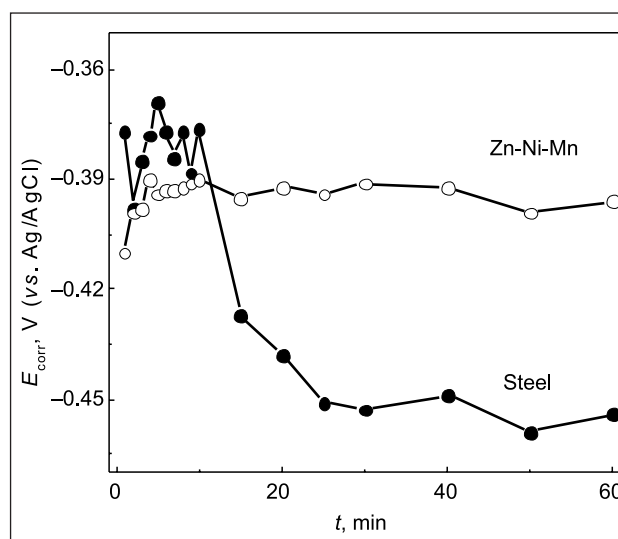


Fig. 4. Dependence of the corrosion potential ( $E_{\text{corr}}$ ) of carbon steel without / with the Zn-Ni-Mn phosphate coating in a sat.  $\text{Ca}(\text{OH})_2 + 1\text{ M NaCl}$  solution on exposure time at  $25\text{ }^\circ\text{C}$

Table 3. Electrochemical parameters of carbon steel with /without Zn-Ni-Mn coating after 1 h immersion in a sat.  $\text{Ca}(\text{OH})_2 + 1 \text{ M NaCl}$  solution, the porosity ( $F$ ) and the protection efficiency of coating ( $P\%$ ) determined from the polarization resistance ( $R_p$ )

| Sample   | $E_{\text{corr}}$ , V (vs. Ag/AgCl) | $b_a$ , mV | $i_{\text{corr}}$ , A $\text{cm}^{-2}$ (Tafel) | $R_p$ , $\text{k}\Omega \text{ cm}^2$ | $F$ , % | $P$ , % |
|----------|-------------------------------------|------------|--|---------------------------------------|---------|---------|
| Steel    | -0.452                              | 78         | $3.2 \cdot 10^{-6}$                            | 3.8                                   | –       | –       |
| Zn-Ni-Mn | -0.391                              | –          | $1.5 \cdot 10^{-7}$                            | 59                                    | ~1.0    | 94      |

monitored during one-hour period. The data obtained have shown that  $E_{\text{corr}}$  values of the samples with the phosphate coating exhibited more positive potential as compared to that of unphosphated substrate.

#### Polarization measurements

The polarization curves of the carbon steel electrode without /with phosphate coating are shown in Fig. 5. The phosphate coating may be considered as an insulating film as it exhibits no electrochemical interaction with the substrate. During the polarization process the properties of substrate material do not change so the anodic process of the coated sample is the same as that of the non-coated one. However, due to the barrier effect of the phosphate coating, the average polarization current declines considerably as compared to the bare steel characteristics. The values of  $i_{\text{corr}}$  and  $R_p$  were determined from polarization measurements and the results obtained are listed in Table 3. For the samples with the Zn-Ni-Mn phosphate coating the values of  $i_{\text{corr}}$  were found to be twenty-fold lower and values of  $R_p$  were seventeen-fold higher with respect to those of bare steel.

The protection efficiency  $P\% = 94\%$  (Table 3) of the phosphate coating was calculated using the following equation [10]:

$$P\% = (R_p - R_{p,m}) / R_p \quad (4)$$

The major problem in using protective coatings, in aggressive environments, is the possible presence of open porosity and pinholes in the coatings [10]. These local defects form direct paths between the corrosive environment and substrate. As the corrosion reactions are initiated at the coating-substrate interface, determination of the porosity is essential in order to estimate the overall corrosion resistance of the coated sample. On the assumption that the phosphate coating is electrochemically inert at low anodic overpotentials, the total porosity rate ( $F$ ) of the coating was calculated using the following equation [19–21]:

$$F = (R_{p,m} / R_p) \times 10^{-|\Delta E_{\text{corr}}| / b_a} \quad (5)$$

where  $R_{p,m}$  is the polarization resistance of bare steel;  $R_p$  is the polarization resistance of phosphated steel;  $\Delta E_{\text{corr}}$  is the difference of  $E_{\text{corr}}$  between steel electrodes with and without phosphate coatings;  $b_a$  is the anodic Tafel slope for bare steel. The carbon steel electrode possessed the following characteristics:  $b_a = 78 \text{ mV}$  and  $R_{p,m} = 3.8 \text{ k}\Omega \text{ cm}^2$  (Table 3).

According to Weng et al. [10], the porosity is directly responsible for the exposed area of substrate at the pores within

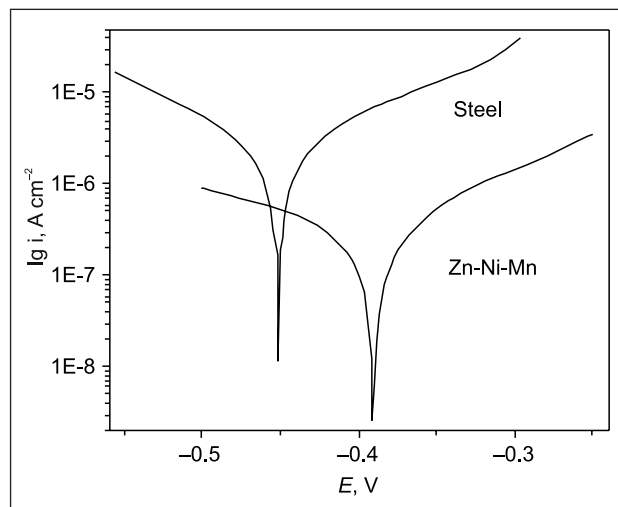


Fig. 5. Potentiodynamic polarization curves of the carbon steel electrodes without /with the phosphate coating measured after immersion in a sat.  $\text{Ca}(\text{OH})_2 + 1 \text{ M NaCl}$  solution for 1 h at  $25 \text{ }^\circ\text{C}$ ;  $0.5 \text{ mV s}^{-1}$

the coating. The calculated mean porosity of the phosphate coating was approximately 1% (Table 3), whereas the  $i_{\text{corr}}$  values of phosphated samples decreased only about twenty-fold as compared to those of bare steel. It means that the steel surface at the bottom of the phosphate coating pores is more active than the surface of bare steel.

The assumption that the mechanism of electrochemical / chemical reaction in pores of the phosphate coating and bare metal is the same is often not verified. The free surface at the bottom of the pores was found to be modified in pre-treatment and post-treatment operations and in some cases was found to be more active than the clean bare metal surface [23]. Furthermore, in the pores of the coating the anodic reaction is the dissolution of iron, and the cathodic reaction is the depolarization of dissolved oxygen. With the hydrolysis of ferrous ions, the electrolyte in the occluded zone is locally acidified. The damage to the coating also begins close to the metal surface. This leads to the penetration of aggressive medium underneath the coating, causing the corrosion of the substrate spreading along the surface. This is called under-film corrosion of phosphated steel in an aqueous solution [10].

#### EIS measurements

EIS measurements were carried out with the aim to determine  $R_p$ , which is in the inverse proportion to  $i_{\text{corr}}$ , and to estimate  $F\%$  of the phosphate coating. The data obtained were fitted and analysed using the EQUIVCRT program of Boukamp [23]. To interpret the EIS data, two equivalent circuit models that are generally used to describe corrosion

processes (Fig. 6) [24, 25] were applied. The calculated parameters of equivalent circuit were used for simulation of impedance diagrams.

The impedance spectra recorded on the carbon steel samples exposed for 1 h to 15 days to the base solution are given in Fig. 7. The electrical parameters obtained for non-phosphated carbon steel through fitting EIS data using an electrical equivalent circuit  $R_{\Omega}(Q_t R_t)$  are listed in Table 4. The proposed electric equivalent circuit is given in Fig. 6a, where  $R_{\Omega} = 1-2 \Omega \text{ cm}^2$  corresponds to the electrolyte resistance between the working and reference electrodes,  $R_t$  represents the charge transfer resistance of steel/solution interface,  $Q_t$  is the constant phase element (CPE). CPE was used instead of a simple capacitor (C) and it is defined by the admittance  $Y$  and the power index number  $n$  [23]:

$$Y = Y_0(j\omega)^n, \quad (6)$$

where  $j$  is the imaginary unit,  $\omega$  is the angular frequency. The term  $n$  shows how far the interface is from the ideal capacitor

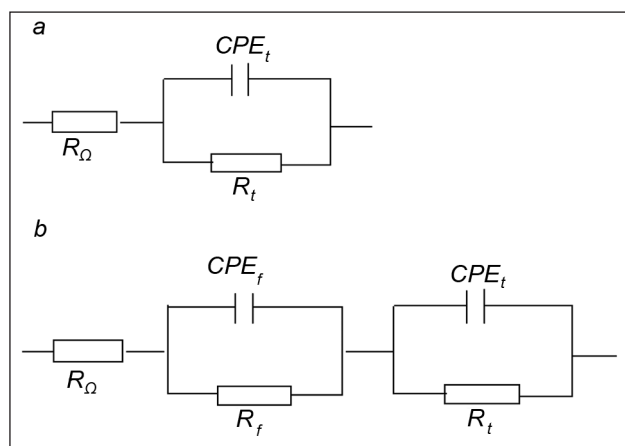


Fig. 6. Equivalent circuits (a) and (b) used for simulation of experimental data.  $R_{\Omega}$  – the resistance of solution;  $R_t$ ,  $CPE_t$  – the charge transfer resistance and the constant phase element;  $R_f$ ,  $CPE_f$  – the passive film electrical resistance of ion transfer through open phosphate coating pores and the constant phase element

(C).  $Y_0(Q)$  becomes  $C$  for  $n = 1$ . The use of the constant phase element is appropriate for the study of electrodes with different heterogeneity and complexity.

The curves (Fig. 7) show a typical set of Bode plots for carbon steel electrode in the base solution. As we can see, the impedance value of bare steel at the lowest frequency decreased with time. The prolongation of the steel exposure to the base solution up to 15 days leads to an approximately two-fold decrease in  $R_t$  values (Table 4).

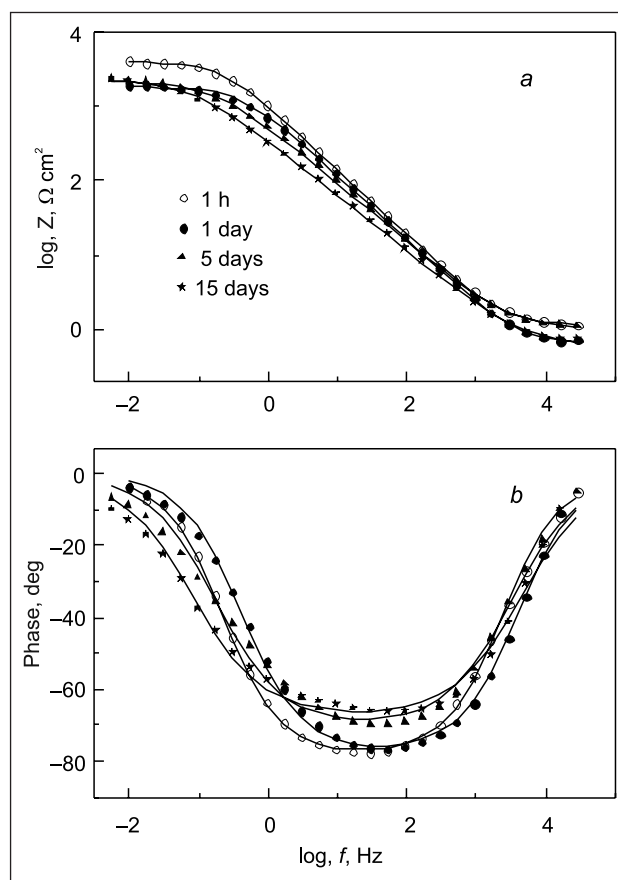


Fig. 7. Bode plots of the impedance spectra after immersion of carbon steel in a sat.  $\text{Ca}(\text{OH})_2 + 1 \text{ M NaCl}$  solution at  $25 \text{ }^\circ\text{C}$

Table 4. Electrochemical impedance spectroscopy parameters obtained by fitting the Bode plots shown in Figs. 7 and 8 with equivalent circuits shown in Fig. 6 for carbon steel without / with the Zn-Ni-Mn coating measured after exposure to a sat.  $\text{Ca}(\text{OH})_2 + 1 \text{ M NaCl}$  solution;  $R_{\Omega} = 1-2 \Omega \text{ cm}^2$

| Sample   | Time, h | $R_t$ , k $\Omega$ cm <sup>2</sup> | $Y_0(Q_t) \times 10^6$ , $\Omega^{-1} \text{ cm}^{-2} \text{ s}^n$ | $n(Q_t)$ | $R_f$ , k $\Omega$ cm <sup>2</sup> | $Y_0(Q_f) \times 10^6$ , $\Omega^{-1} \text{ cm}^{-2} \text{ s}^n$ | $n(Q_f)$ | $^*R_p$ , k $\Omega$ cm <sup>2</sup> | $\chi^2$ (error factor) | $F$ , % |
|----------|---------|------------------------------------|--|----------|------------------------------------|--|----------|--------------------------------------|-------------------------|---------|
| Steel    | 1       | 4                                  | 185  | 0.88     | –                                  | –  | –        | 4                                    | 0.0041                  | –       |
| " "      | 2       | 3.8                                | 181  | 0.88     | –                                  | –  | –        | 3.8                                  | 0.0063                  | –       |
| " "      | 5       | 2.4                                | 184  | 0.89     | –                                  | –  | –        | 2.4                                  | 0.0032                  | –       |
| " "      | 24      | 1.9                                | 235  | 0.87     | –                                  | –  | –        | 1.9                                  | 0.0051                  | –       |
| " "      | 120     | 2.2                                | 417  | 0.78     | –                                  | –  | –        | 2.2                                  | 0.0038                  | –       |
| " "      | 360     | 2.4                                | 698  | 0.75     | –                                  | –  | –        | 2.4                                  | 0.0046                  | –       |
| Zn-Ni-Mn | 1       | 2.2                                | 38   | 0.54     | 54.7                               | 8.1  | 0.72     | 56.9                                 | 0.0051                  | ~1      |
| " "      | 120     | 2.6                                | 113  | 0.56     | 57.1                               | 16.4   | 0.63     | 64.7                                 | 0.0074                  | –       |
| " "      | 360     | 1.5                                | 301.4  | 0.61     | 79.4                               | 19.2   | 0.62     | 80.9                                 | 0.0066                  | –       |
| " "      | 960     | 3.1                                | 506.6  | 0.7      | 66                                 | 40.4   | 0.61     | 69.1                                 | 0.0078                  | –       |

$^*R_p = R_t + R_f$

Impedance spectra recorded for carbon steel samples with the Zn-Ni-Mn phosphate coating after exposure to the base solution for 1 h to 40 days are given in Fig. 8. An exposure of the phosphated samples to the base solution led to a great increase in impedance values and a clear appearance of the second capacitive time constant. Therefore, to simulate corrosion processes in the coated system, the  $R_0(QR_f)(QR_t)$  circuit (Fig. 6b) was used. The first in series  $R_f$ - $CPE_f$  combination should represent the resistance and capacitance of the phosphate coating, where  $R_f$  is the electrical resistance of ion transfer through the open coating pores in parallel with coating capacitance. The second  $R_t$ - $CPE_t$  is related to the electrochemical properties of the corroding steel electrode. The fitting parameters are listed in Table 4.

The comparison of EIS measurements data (Table 4) shows that after 1 h of immersion in the base solution the charge transfer resistance  $R_t$  values of phosphated samples were about twofold lower as compared to that of bare steel. It suggests that the steel surface at the bottom of the phosphate coating pores is more active than that of bare steel.

The polarization resistance  $R_p$  values are the sum of the pore resistance ( $R_f$ ) and the charge transfer resistance ( $R_t$ ). After 1 h of exposure to the base solution the phosphated samples possessed about fifteen-fold higher  $R_p$  values as compared to those obtained for bare steel. The value of porosity of the phosphate coating was calculated on the basis of

determined electrochemical parameters using Eq. (5). It has been established that the porosity of coating was in the order of 1%. The porosity rate values obtained by the EIS technique (Table 4) are in total agreement with the value evaluated by linear polarization measurements (Table 3). A low value of porosity is beneficial to the corrosion resistance of the coating that acts as a physical barrier against corrosive agents. In general, a lower porosity means a lower corrosion rate of the substrate [10]. The prolongation of exposure time up to 15 days leads to an approximately twofold decrease in  $R_p$  values of bare steel, while the phosphated samples possessed about thirty-fold higher  $R_p$  values as compared to those obtained for bare steel. As the results obtained after 40 days of exposure demonstrate (Table 4), the total impedance value of the phosphated samples did not decrease but possessed about 70–80  $k\Omega\text{ cm}^2$ . This increase in  $R_p$  values could be explained by the fact that the base solution reached the steel surface through the pores, which resulted in the deposition of corrosion products in the phosphate coating pores.

To summarize the results of electrochemical and SEM measurements, the low porosity (1%) medium weight crystalline Zn-Ni-Mn phosphate coating on carbon steel demonstrated effective protective properties in a chloride-contaminated alkaline solution.

## CONCLUSIONS

The gravimetric and SEM studies have shown that the Zn-Ni-Mn phosphate coating (0.4 at.% of Ni and 1.1 at.% of Mn) formed on carbon steel was medium weight (1.9–3.4  $\text{g m}^{-2}$ ) with the thickness of  $\sim 2\ \mu\text{m}$ . According to XRD analysis data the conversion coating was composed of three phases: hopeite  $\text{Zn}_3(\text{PO}_4)_2 \cdot 4\text{H}_2\text{O}$ , phosphophyllite  $\text{Zn}_2\text{Fe}(\text{PO}_4)_2 \cdot 4\text{H}_2\text{O}$  and Fe.

The results of electrochemical measurements revealed that after immersion into a saturated  $\text{Ca}(\text{OH})_2 + 1\ \text{M NaCl}$  solution for 1 h the corrosion current of phosphated samples decreased about twenty-fold, and the polarization resistance  $R_p$  increased seventeen-fold as compared to those of the substrate. The prolongation of exposure time from 1 h up to 15 days leads to an approximately thirty-fold increase in  $R_p$  values of the phosphated samples as compared to those obtained for bare steel.

The estimated porosity of the Zn-Ni-Mn phosphate coating was approximately 1%. The porosity values measured using the two techniques, EIS and linear polarization, were in agreement.

The EIS measurements data show that after 1 h of immersion in the base solution the charge transfer resistance  $R_t$  values of phosphated samples were about twofold lower as compared to those of substrate. It suggests that the steel surface at the bottom of the phosphate coating pores is more active than that of bare steel.

To summarize the results of electrochemical and SEM measurements, the low porosity medium weight crystalline

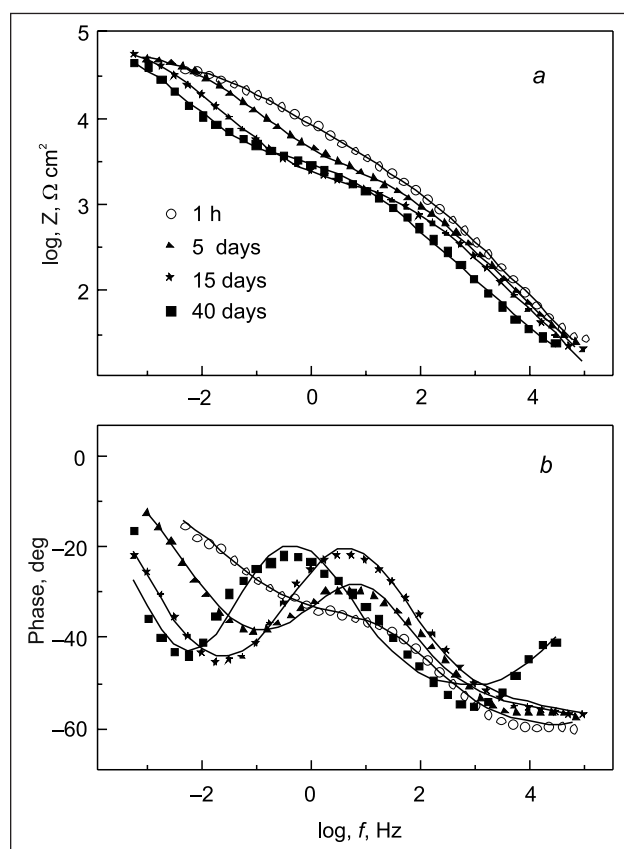


Fig. 8. Bode plots of the impedance spectra after immersion of the phosphated carbon steel in a sat.  $\text{Ca}(\text{OH})_2 + 1\ \text{M NaCl}$  solution at 25 °C

Zn-Ni-Mn phosphate coating on carbon steel demonstrated effective protective properties in a chloride-contaminated alkaline solution.

## ACKNOWLEDGEMENTS

This research was supported by the Research Council of Lithuania under Grant No. MIP-77/2010. The authors thank Dr. A. Selskis (Centre for Physical Sciences and Technology, Institute of Chemistry) for his assistance performing SEM measurements, Dr. R. Juškėnas (Centre for Physical Sciences and Technology, Institute of Chemistry) for his assistance performing XRD measurements.

Accepted 26 March 2013

Received 16 May 2013

## References

- M. M. Jalili, S. Moradian, D. Hosseinpour, *Constr. Build. Mater.*, **23**, 233 (2009).
- F. Simescu, H. Idrissi, *Corr. Sci.*, **51**, 833 (2009).
- S. R. Yeomans, *Corrosion*, **50**, 72 (1994).
- M. Manna, *Corr. Sci.*, **51**, 451 (2009).
- D. B. Freeman, *Phosphating and Metal Pre-Treatment*, Woodhead-Faulkner Ltd., Cambridge, England (1986).
- U. B. Nair, *Met. Finish.*, **93**, 40 (1995).
- P. K. Sinha, R. Feser, *Surf. Coat. Technol.*, **161**, 158 (2002).
- I. S. Leea, H. E. Kim, S. Y. Kim, *Surf. Coat. Technol.*, **131**, 181 (2001).
- J. Flis, J. Mankowski, T. Bell, T. Zakroczymski, *Corros. Sci.*, **43**, 1711 (2001).
- D. Weng, P. Jokiel, A. Uebleis, H. Boehni, *Surf. Coat. Technol.*, **88**, 147 (1996).
- W. Paatsch, W. Kautek, M. Sahre, *Trans. Inst. Met. Finish.*, **75(6)**, 216 (1997).
- D. Zimmermann, A. G. Munoz, J. W. Schultze, *Electrochim. Acta*, **48**, 3267 (2003).
- J. Donofrio, *Met. Finish.*, **98**, 57 (2000).
- M. F. Morks, *Mater. Lett.*, **58**, 3316 (2004).
- W. A. Roland, K. H. Gottwald, *Metalloberfläche*, **42**, 301 (1988).
- K. Ogle, A. Tomandl, N. Meddahi, M. Wolpers, *Corr. Sci.*, **46**, 979 (2004).
- A. Tomandl, M. Wolpers, K. Ogle, *Corr. Sci.*, **46**, 997 (2004).
- W. Machu, *Die Phosphatierung*, Verlag Chemie, Weinheim (1950).
- V. F. C. Lins, G. F. A. Reis, C. R. Araujo, T. Matencio, *Appl. Surf. Sci.*, **253**, 2875 (2006).
- J. Creus, H. Mazille, H. Idrissi, *Surf. Coat. Technol.*, **130**, 224 (2000).
- C. Liu, Q. Bi, A. Leyland, A. Matthews, *Corr. Sci.*, **45**, 1257 (2003).
- B. D. Cullity, *Elements of X-Ray Diffraction*, 2nd ed., Addison-Wesley Publishing Company, Philippines (1978).
- B. A. Boukamp, *J. Electrochem. Soc.*, **142**, 1885 (1995).
- L. Freire, X. R. Nóvoa, M. F. Montemor, M. J. Carmezim, *Mater. Chem. Phys.*, **114**, 962 (2009).
- El-Sayed M. Sherif, R. M. Erasmus, J. D. Comins, *Electrochim. Acta*, **55**, 3657 (2010).

O. Girčienė, R. Ramanauskas, L. Gudavičiūtė, A. Martušienė

## KONVERSINĖS Zn-Ni-Mn FOSFATINĖS DANGOS FORMAVIMAS ANT PLIENO BEI FOSFATUOTŲ BANDINIŲ KOROZINĖ ELGSENA CHLORIDAIS UŽTERŠTUOSE ŠARMINIUOSE TIRPALUOSE

### Santrauka

Ištirta cheminių Zn-Ni-Mn fosfatinių dangų formavimo ant anglinio plieno dėsningumai bei fosfatuotų bandinių elgsena chloridais užterštuose šarminiuose tirpaluose. Fosfatinių dangų cheminė sudėtis ir morfologija buvo tirtos naudojant rentgeno spindulių difrakcinės (XRD) analizės ir skenuojančios elektronų mikroskopijos (SEM) metodus. Nustatyta, kad kristalinė Zn-Ni-Mn fosfatinė danga (0,4 at. % Ni ir 1,1 at. % Mn) yra ~2 μm storio, vidutinės masės (1,9–3,4 g m<sup>-2</sup>) ir sudaryta iš trijų fazių: hopeito Zn<sub>3</sub>(PO<sub>4</sub>)<sub>2</sub> · 4H<sub>2</sub>O, fosfofilito Zn<sub>2</sub>Fe(PO<sub>4</sub>)<sub>2</sub> · 4H<sub>2</sub>O ir Fe. Atlikti elektrocheminiai matavimai parodė, kad išlaikius 1 val. sotaus Ca(OH)<sub>2</sub> + 1 M NaCl tirpale Zn-Ni-Mn bandinių korozijos srovių vertės (*i*<sub>corr</sub>) yra 20 kartų mažesnės, o poliarizacinių varžų (*R*<sub>p</sub>) vertės – 17 kartų didesnės nei plieninių bandinių. Prailginus išlaikymo laiką tirpale iki 15 parų, fosfatuotų bandinių *R*<sub>p</sub> vertės buvo apie 30 kartų didesnės nei anglinio plieno. Nustatyta, kad mažo poringumo (~1 %) kristalinė Zn-Ni-Mn fosfatinė danga, nusodinta ant anglinio plieno, pasižymi geromis apsauginėmis savybėmis šarminiam chloridais užterštam tirpale.